Available online at www.sciencedirect.com
ScienceDirect
European Journal of Pharmaceutics and Biopharmaceutics 67 (2007) 141–148
European Journal of Pharmaceutics and Biopharmaceutics
www.elsevier.com/locate/ejpb

Research paper

Cetyl palmitate-based NLC for topical delivery of Coenzyme Q_{10} – Development, physicochemical characterization and *in vitro* release studies

Veerawat Teeranachaideekul [a,b], Eliana B. Souto [b], Varaporn B. Junyaprasert [a], Rainer H. Müller [b,*]

[a] *Department of Pharmacy, Mahidol University, Bangkok, Thailand*
[b] *Department of Pharmaceutics, Biopharmaceutics and Quality Management, Free University of Berlin, Berlin, Germany*

Received 30 August 2006; accepted in revised form 17 January 2007
Available online 30 January 2007

Abstract

In the present study, nanostructured lipid carriers (NLC) composed of cetyl palmitate with various amounts of caprylic/capric triacylglycerols (as liquid lipid) were prepared and Coenzyme Q_{10} (Q_{10}) has been incorporated in such carriers due to its high lipophilic character. A nanoemulsion composed solely of liquid lipid was prepared for comparison studies. By photon correlation spectroscopy a mean particle size in the range of 180–240 nm with a narrow polydispersity index (PI) lower than 0.2 was obtained for all developed formulations. The entrapment efficiency was 100% in all cases. The increase of oil loading did not affect the mean particle size of NLC formulations. NLC and nanoemulsion, stabilized by the same emulsifier, showed zeta potential values in the range −40/−50 mV providing a good physical stability of the formulations. Scanning electron microscopy studies revealed NLC of disc-like shape. With respect to lipid polymorphism, a decrease in the ordered structure of NLC was observed with the increase of both oil and Q_{10} loadings, allowing therefore high accommodation for Q_{10} within the NLC. Using static Franz diffusion cells, the *in vitro* release studies demonstrated that Q_{10}-loaded NLC possessed a biphasic release pattern, in comparison to Q_{10}-loaded nanoemulsions comprising similar composition of which a nearly constant release was observed. The NLC release patterns were defined by an initial fast release in comparison to the release of NE followed by a prolonged release, which was dependent on the oil content.

Keywords: Nanostructured lipid carriers; NLC; Coenzyme Q_{10}; Cetyl palmitate; *In vitro* release

1. Introduction

During the last decade, several new drug carrier systems which can control drug release as well as drug targeting have been extensively developed. Such examples are nanoemulsions (NE), nanosuspensions (NS), liposomes, polymeric nanoparticles, self-emulsifying drug delivery systems (SEDDS), solid lipid nanoparticles (SLN) and nanostructured lipid carriers (NLC) [1–7]. SLN have been introduced as an alternative carrier for nanoemulsions, liposomes and polymeric nanoparticles. SLN combine many advantages of such colloidal carriers, e.g. controlled drug release, biocompatibility and drug targeting. They can also be produced on large scale using the high pressure homogenization (HPH) technique. In previous reports, many drugs have been successfully incorporated into SLN [8–10]. However, some problems also occurred including low drug loading and drug expulsion from the carrier during storage time owing to polymorphic transformations during the shelf life of such systems. These problems arise from the composition of solid lipids, which generally are pure lipids and/or a blend of solid lipids. After production by HPH technique, the lipid particles crystallize in

* Corresponding author. Department of Pharmaceutics, Biopharmaceutics and Quality Management, Free University of Berlin, Kelchstr. 31, D-12169 Berlin, Germany. Tel.: +49 30 83850678; fax: +49 30 83850616.
E-mail address: mpharma@zedat.fu-berlin.de (R.H. Müller).

0939-6411/$ - see front matter © 2007 Elsevier B.V. All rights reserved.
doi:10.1016/j.ejpb.2007.01.015

metastable polymorphic forms of high energy (i.e. low thermodynamic stability). With respect to thermodynamic aspects, the system transforms into a more stable system reducing its free energy and therefore showing a high degree of order. This leads to a reduction of imperfections in the crystal lattice of the lipids. This phenomenon occurs faster in case of pure lipids compared to mixtures of lipids. When this happens, drug molecules can be expelled from the carrier, which leads to an uncontrolled release and to a decrease of the chemical stability of such molecules. Therefore, to decrease the degree of organization of lipid matrix in SLN, as well as to increase the drug loading, NLC have been developed and reported as the second generation of lipid nanoparticles [3,11]. Based on the chemical nature of the lipid molecules, the inner structure of NLC is different from that of SLN because the former is composed of mixtures of solid and liquid lipids (oils). The solubility of active ingredients in oils is generally much higher than in solid lipids. For that reason, the higher loading capacity could be achieved by the development of NLC. With this approach, drug expulsion during storage time is also minimized. Admixture of liquid with solid lipids leads to the creation of a less ordered inner structure. Thus, the drug molecules can be accommodated in between lipid layers and/or fatty acid chains [3].

From the literature reviews there are several methods to produce lipid nanoparticles such as microemulsion techniques, solvent evaporation in o/w emulsion, solvent displacement technique, solvent diffusion technique and HPH technique [1,12,13]. However, HPH technique shows many advantages compared to the other methods, e.g. scale up possibility, avoidance of organic solvents and short production time. In addition, depending on the chemical nature of lipids and surfactant concentrations HPH allows the modification of drug release profiles from the carriers by modifying the production parameters such as temperature, number of cycles and homogenization pressure [1,13].

Coenzyme Q_{10} (Q_{10}) is known as an endogenous cellular antioxidant. It is composed of a long side chain containing ten isoprenoid units. Due to its structure, the aqueous solubility is very low, causing a low oral bioavailability. In terms of cosmetic applications, this active has shown the ability to reduce photoaging *in vivo* with a corresponding decrease in wrinkle depth [14].

From previous studies it has been observed that the production method influences the release profile of the drug entrapped into the lipid matrix [13]. NLC based on stearic acid and oleic acid prepared by solvent diffusion method showed the occurrence of burst release at the initial release depending on the amount of oil loading [15], whereas NLC prepared by HPH technique based on glyceryl behenate and various amounts of caprylic/capric triacylglycerols showed that the increase of the release rate was due to lipid modification leading to drug expulsion with time [8,16]. Therefore, the aim of this study was the investigation of the effect of increasing the oil loading and Q_{10} on the physicochemical properties of NLC based on cetyl palmitate and caprylic/capric triacylglycerols. Particle size, zeta potential and degree of crystallinity of NLC, as well as the entrapment efficiency of Q_{10} into the carriers and its *in vitro* release assessed by Franz diffusion cells, were evaluated in comparison to a nanoemulsion (NE) of similar composition produced under the same conditions.

2. Materials and methods

2.1. Materials

Precifac® ATO (cetyl palmitate), Labrasol® (PEG-8 caprylic/capric triacylglycerols) and Miglyol® 812 (caprylic/capric triacylglycerols) were purchased from Gattefossé (Cedex, France). Tego® Care 450 (Polyglyceryl-3 methylglucose distearate) was purchased from Goldschmidt (Essen, Germany). Q_{10} was from Sigma–Aldrich (Deisenhofen, Germany). Methanol and tetrahydrofuran were obtained from Merck (Darmstadt, Germany). Ultrapurified water was obtained from a MilliQ Plus system, Millipore (Schwalbach, Germany).

2.2. Preparation of NLC and NE

NLC containing 24% of Q_{10} based on the lipid content and Q_{10}-free NLC were produced by hot HPH (Micron LAB40, Homogenizer Systems, Germany). Briefly, the melted lipid phase containing solid lipid, liquid lipid and active was dispersed in a hot surfactant solution (85 °C), obtaining a pre-emulsion by high speed stirring using an Ultra-Turrax T25 (Janke and Kunkel GmbH, Staufen, Germany) at 8000 rpm for 1 min. This hot pre-emulsion was further processed by HPH applying three homogenization cycles at 500 bar and 85 °C. The lipid dispersion was cooled at ambient conditions to room temperature and solidified to obtain the aqueous NLC dispersions.

In case of nanoemulsions, these were produced in the same manner at 85 °C as the NLC dispersion, however, the solid lipid (cetyl palmitate) was replaced by Miglyol® 812 [caprylic/capric triacylglycerols (TAG)]. The composition of all formulations is shown in Table 1.

2.3. Particle size

Particle size analysis was performed by photon correlation spectroscopy (PCS) with a Malvern Zetasizer IV (Malvern Instruments, UK). PCS yields the mean particle size (z-ave) and the polydispersity index (PI) which is a measure of the width of the size distribution. The z-ave and PI values were obtained being the average of 10 measurements at an angle of 90° in 10 mm diameter cells at 25 °C. Prior to the measurement all samples were diluted with bidistilled water to have a suitable scattering intensity. The real refractive index and the imaginary refractive index were set at 1.456 and 0.01, respectively. The particle size analysis was determined using the Mie theory. To detect the possible presence of microparticles, the laser diffractometry

Table 1
Compositions of the developed NLC and NE formulations % (w/w)

Formulations	Cetyl palmitate	Miglyol® 812	Tego® Care 450	Q_{10}	Water q.s.
Q_{10}-free NLC1	9.50	0.50	1.8	–	100
Q_{10}-loaded NLC 1	7.23	0.38	1.8	2.4	100
Q_{10}-loaded NLC 2	6.84	0.76	1.8	2.4	100
Q_{10}-loaded NLC 3	6.46	1.14	1.8	2.4	100
Q_{10}-free NLC 4	19.00	1.00	1.8	–	100
Q_{10}-loaded NLC 4	14.45	0.75	1.8	4.8	100
Q_{10}-free NE1	–	10.00	1.8	–	100
Q_{10}-loaded NE1	–	7.60	1.8	2.4	100

(LD) (Coulter®LS 230, Beckmann–Coulter Electronics, Krefeld, Germany) with polarization intensity differential scattering (PIDS) was applied. The LD data obtained were evaluated using volume distribution as diameter (d) values of 10%, 50%, 90% and 99% and Span values. The diameter values indicate the percentage of particles possessing a diameter equal to or lower than the given value. The Span value is a statistical parameter useful to evaluate the particle size distribution and calculated applying the following equation:

$$\text{Span} = \frac{d90\% - d10\%}{d50\%} \quad (1)$$

2.4. Zeta potential

The zeta potential (ZP), reflecting the electric charge on the particle surface and indicating the physical stability of colloidal systems, was measured by determining the electrophoretic mobility using the Malvern Zetasizer IV. The measurements were performed in bidistilled water adjusted to a conductivity of 50 μS/cm with sodium chloride solution (0.9% w/v). The ZP was calculated using the Helmholtz–Smoluchowsky equation. The pH was in the range of 5.5–6.0 and the applied field strength was 20 V/cm.

2.5. Scanning electron microscopy

Scanning electron microscopy (SEM) was applied to investigate the morphological characteristics (shape and surface structure) of Q_{10}-loaded NLC. The samples were analysed using the scanning electron microscope equipped with a field emission, a JSM 6301F (JEOL, Japan) after coating the samples with gold using a Gold coater JFC 1200 fine coater (JEOL, Japan). Prior to analysis, samples were diluted with bidistilled water, dropped on the amorphous carbon grid, and then air-dried at room temperature.

2.6. Determination of encapsulation efficiency

The encapsulation efficiency (E.E.) of Q_{10} into NLC and NE was determined indirectly by ultrafiltration method using centrifugal filter tubes (Amicon Ultra-4, Millipore, Ireland) with a 30 kDa molecular weight cut-off. The amount of encapsulated active was calculated by the difference between the total amount used to prepare the systems and the amount of Q_{10} that remained in the aqueous phase after isolation of the systems, applying Eq. (2):

$$\text{E.E.} = \frac{\text{Total amount of } Q_{10} - \text{Free amount of } Q_{10}}{\text{Total amount of } Q_{10}} \quad (2)$$

Analysis of Q_{10} was performed by HPLC at the wavelength of 280 nm on a Kroma System 2000 (Kontron Instruments, Berlin, Germany) running in the isocratic mode. Kontron HPLC software was used to perform integration of the peaks. The system consisted of a Bondapak® C18 RP column (Water, Ireland). The mobile phase consisted of 90 parts of methanol and 10 parts of tetrahydrofuran. The injection volume was 20 μl, the flow rate 1.5 ml/min. The running time was 10 min.

2.7. Differential scanning calorimetry (DSC)

To evaluate lipid crystallinity and polymorphism, thermal behaviour studies were performed using a Mettler DSC 821e apparatus. The samples weighing approximately 1–3 mg based on the lipid content were placed in 40 μl aluminium pans. An empty aluminium pan was used as a reference. The heating runs were performed from 25 to 85 °C and cooled to 0 °C using the heating rate of 5 K/min by flushing with nitrogen at the rate of 80 ml/min. The melting point, enthalpies (ΔH) and onset temperatures were evaluated using the STAR^e Software (Mettler Toledo, Switzerland). The determination of crystallinity index was calculated using Eq. (3):

$$\text{CI}(\%) = \frac{\Delta H_{\text{NLC aqueous dispersion}}}{\Delta H_{\text{bulk material}} \times \text{Concentration}_{\text{lipid phase}}} \times 100 \quad (3)$$

2.8. X-ray diffraction

Wide-angle X-ray scattering (WAXS) investigations were performed by a Philips PW1830 X-ray generator (Philips, Amedo, the Netherlands) with a copper anode (Cu-Kα radiation, 40 kV, 25 mA, $\lambda = 0.15418$ nm), using a Goniometer PW18120 as a detector. The measurements were analysed at 2 Theta from 0.6° to 40.0°. Bragg's equation was used to transform the data from scattering angle to the spacings of lipid chains. Prior to measurement, 0.6 ml

of Q_{10}-loaded NLC dispersions was admixed with 0.2 g of locust bean gum powder to produce a paste, and then mounted into a glass fibre. The data used were typically collected with a step width of 0.04° and a count time of 60 s.

2.9. In vitro release studies

Static Franz diffusion cells (Crown Scientific, Sommerville, USA) were used to evaluate the amount of drug release from the developed formulations. The surface area of the release membrane was 0.64 cm^2 and the volume of the receptor phase was approximately 6 ml. The temperature of the assay was accurately controlled at 32 °C to mimic human skin. Cellulose acetate membrane filters having a pore size diameter of 50 nm (VMTE 0.05 μm, Millipore, Germany) were used as a membrane and mounted on the Franz diffusion cells. The acceptor medium was composed of an aqueous solution of 5% Labrasol® (pH 5), stirred by magnetic bar at 700 rpm to avoid different concentrations within the acceptor medium and to minimize stagnant layers. 100 μl of aqueous NLC and NE dispersions was placed onto the membrane in the donor compartment. Samples of 500 μl were withdrawn at suitable time intervals over 24 hr using a syringe needle, and the same volumes were replaced with freshly prepared acceptor medium. The samples were analysed by HPLC as previously described. The experiment was done in triplicate.

2.10. Statistics

The data are present mean values ± standard deviation (SD). Significance of difference was evaluated using Student's *t*-test and one-way ANOVA at the probability level of 0.05.

3. Results and discussion

3.1. Particle size and zeta potential analysis

Aqueous NLC dispersions composed of 10% lipid phase (solid lipid, liquid lipid and Q_{10}) were prepared using different ratios between solid lipid and liquid lipid, i.e. 95:5, 90:10 and 85:15 (Table 1). To investigate the influence of lipid concentration, NLC composed of 20% lipid phase at the ratio of 95:5 were prepared. Table 2 shows the mean particle size (z-ave) of NE and NLC evaluated by PCS. After loading Q_{10} within the developed systems, the mean particle size did not increase significantly in the case of NLC ($p > 0.05$). However, with regard to NE, the size increased significantly ($p < 0.05$) after their loading with Q_{10}. The increase in oil content did not increase the particle size of Q_{10}-loaded NLC ($p > 0.05$). Comparing the z-ave values of NE and NLC, it was found that NE showed a smaller particle size than NLC both before and after loading the systems with Q_{10}. This is similar to that reported for SLN [17]. This result might be due to the anisometric shaped particles of NLC. When comparing the diffusion coefficient (D) in the same volume of spherical and anisometric shaped particles, NE shows higher D values in comparison to NLC. This effect has an impact on the particle size calculated by the Stokes–Einstein equation. Moreover, the higher concentration of lipid phase, the higher mean particle sizes will be obtained. PI values were lower than 0.2 for all formulations indicating a relatively narrow size distribution especially in the case of Q_{10}-free NLC4 (Table 2), which are composed of 20% of lipid phase. Due to the limitation of PCS (which can measure the particles from a few nm to 3 μm), LD was performed to detect the presence of microparticles. Table 3 shows that the obtained volume distribution diameter of 99% particles was lower than 450 nm. The narrow size distribution reported previously was confirmed by the Span values, i.e. the lower the Span the narrower is the particle size distribution.

Table 2
Mean particle size (z-ave), polydispersity index (PI) and zeta potential values of NE and NLC formulations determined by PCS (25 °C) on the day of production

Formulations	z-ave[a]	PI[a]	ZP[b] (mV)
Q_{10}-free NLC1	192.5 ± 2.6	0.117 ± 0.034	−43.8 ± 0.9
Q_{10}-loaded NLC 1	195.9 ± 3.6	0.128 ± 0.058	−45.7 ± 0.8
Q_{10}-loaded NLC 2	195.1 ± 2.7	0.173 ± 0.059	−42.9 ± 1.3
Q_{10}-loaded NLC 3	196.5 ± 3.2	0.133 ± 0.064	−41.7 ± 1.3
Q_{10}-free NLC 4	226.7 ± 2.6	0.069 ± 0.053	−44.8 ± 0.9
Q_{10}-loaded NLC 4	238.3 ± 3.8	0.103 ± 0.062	−45.5 ± 1.3
Q_{10}-free NE1	180.8 ± 3.1	0.129 ± 0.049	−48.7 ± 0.7
Q_{10}-loaded NE1	187.0 ± 3.0	0.127 ± 0.050	−48.3 ± 0.7

[a] Mean of $n = 10$ measurements.
[b] Mean of $n = 5$ measurements.

The analysis of the ZP, which is the electric potential at the plane of shear, is a useful tool to predict the physical storage stability of colloidal systems. The nanoparticles had the higher ZP value, indicating the better stability of this colloidal system [1]. ZP values higher than −30 mV show good physical stability, being optimized when they reach approximately −60 mV, exhibiting a very good physical stability during the shelf-life. In the present study, the ZP values of all formulations were in the range −40 mV/−50 mV (Table 2), showing that both NE and NLC should possess a good physical stability since particle aggregation is not likely to occur owing to electrostatic repulsion

Table 3
Volume distribution diameters in micrometer (μm) ($d10\%$, $d50\%$, $d90\%$ and $d99\%$) and Span values obtained by LD on the day of production

Formulations	$d10\%$	$d50\%$	$d90\%$	$d99\%$	Span
Q_{10}-free NLC1	0.074	0.128	0.214	0.286	1.094
Q_{10}-loaded NLC 1	0.073	0.128	0.219	0.296	1.140
Q_{10}-loaded NLC 2	0.071	0.123	0.214	0.292	1.163
Q_{10}-loaded NLC 3	0.072	0.124	0.216	0.296	1.161
Q_{10}-free NLC 4	0.107	0.170	0.254	0.322	0.865
Q_{10}-loaded NLC 4	0.089	0.186	0.311	0.409	1.196
Q_{10}-free NE1	0.079	0.137	0.220	0.284	1.029
Q_{10}-loaded NE1	0.082	0.143	0.231	0.303	1.042

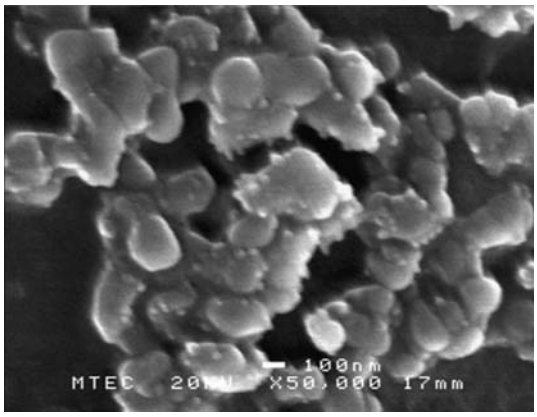

Fig. 1. SEM image of Q_{10}-loaded NLC1.

between the particles. In addition, the steric hindrance from the stabilizer will have an additional effect increasing the particle stability.

3.2. Scanning electron microscopy (SEM)

To obtain more information about the particle size and shape, SEM analysis was also performed. Fig. 1 shows the image of Q_{10}-loaded NLC1. As expected, particles revealed an anisometric shape with a size of approximately 200 nm. The picture depicts agglomeration of individualized particles due to lipid nature of the carriers and sample preparation prior to SEM analysis. In previous reports, non-spherical shapes of SLN and NLC were reported using transmission electron microscopy (TEM) technique [18] and cryo-TEM [19]. Using cryo-field emission SEM (cryo-FESEM) it has been recently reported that the particle shape of SLN and NLC was almost spherical [19]. Therefore, particle shape deviation from sphericity might be due to the lipid modification during drying process of sample treatment. In addition, the particle shape depends on the purity of the lipid. Highly pure tristearin particles are more cuboid [20]. Particles from much less pure cosmetic lipid (i.e. chemically polydispersed lipids) show a perfect spherical shape as shown by atomic force microscopy (AFM) [21].

3.3. Encapsulation efficiency

From the recent literature, several drugs have been successfully entrapped in NE, SLN and NLC, e.g. tetracaine, etomidate, mifepristone, clotrimazole, ascorbyl palmitate, and retinol [11,22–26]. When comparing the encapsulation parameters between SLN and NLC, it was reported that NLC show a higher drug loading capacity and encapsulation efficiency (E.E.) than SLN [11,25]. Moreover, when increasing the amount of oil in NLC, it was found that the percentage of encapsulated drug increases [15]. This is due to the fact that the majority of lipophilic drugs solubilize better in oils than in solid lipids. In addition, the number of imperfections in the particle matrix increases, providing space for the accommodation of drugs. To assess the encapsulation parameters in colloidal carriers such as lipid nanoparticles, previous separation of the systems from the aqueous external phase is required. This can be performed by ultracentrifugation and/or ultrafiltration techniques. Ultracentrifugation methods require application of centrifugal force for the separation of the nanoparticles from the aqueous medium, which might possibly destroy the carriers. In case of NE, the density of the oil droplets is lower than that of the water. Therefore, ultrafiltration technique was selected as a procedure for separation. Encapsulation efficiency was calculated using Eq. (2). Once Q_{10} is not detected in the ultrafiltrate, it can be assumed that incorporation of Q_{10} into NE and NLC was approximately 100% (the limit of detection (LOD) was found to be 125 ng/ml). In the present study, no Q_{10} was detected in the ultrafiltrate of all formulations. Moreover, the drug crystals could not be observed by polarized light microcopy (data not shown). Thus, it can be deduced that 100% E.E. was assumed in all formulations. This result is due to the high lipophilicity of Q_{10}, the high solubility of the active both in the oil (Miglyol®812) and in the wax (cetyl palmitate), in addition to its low solubility in water (solubility of Q_{10} in water = 4 ng/ml) [27]. However, Q_{10}-loaded nanoparticles produced via microemulsion technique showed an E.E. of about 74%, most likely due to the type and the amount of surfactant used to stabilize the systems [28]. From the obtained results, optimized NLC and NE formulations were produced by HPH technique for the delivery of Q_{10}.

3.4. DSC investigations

To characterize the polymorphism and the degree of crystallinity of the lipid nanoparticles, DSC has been performed (Table 4). The obtained results have further been correlated with the encapsulation parameters, release profiles, and physical stability of these carriers. The melting point of nanoparticles was lower than that of the bulk material (<52 °C), but higher than 40 °C, which is the prerequisite for topical application of lipid carriers. Cetyl palmitate revealed two peaks at 43.08 and 52.82 °C reflecting two distinct polymorphic forms (Fig. 2). From the literature reviews, the one with lower melting point is attributed to the α polymorphic form, whereas the latter

Table 4
DSC parameters of Q_{10}-free and of Q_{10}-loaded NLC obtained on the day of production

Formulations	Melting point (°C)	Onset (°C)	Enthalpy (J/g)	CI (%)
Q_{10}-free NLC1 (5% oil)	49.34	45.86	19.98	89.66
Q_{10}-loaded NLC 1 (5% oil)	47.79	45.04	14.39	64.58
Q_{10}-loaded NLC 2 (10% oil)	47.36	44.76	14.29	64.13
Q_{10}-loaded NLC 3 (15% oil)	47.32	44.90	12.45	55.87
Q_{10}-free NLC 4 (5% oil)	49.65	47.29	43.07	96.64
Q_{10}-loaded NLC 4 (5% oil)	48.30	45.36	31.49	70.36

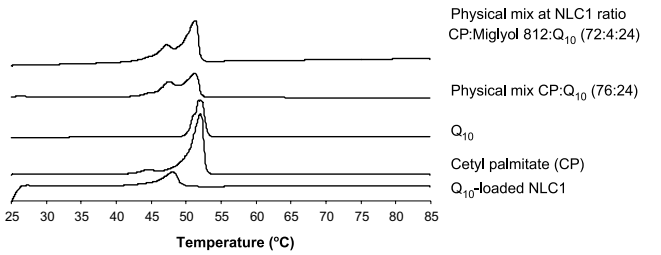

Fig. 2. DSC curves of bulk materials, physical mixtures and NLC dispersions.

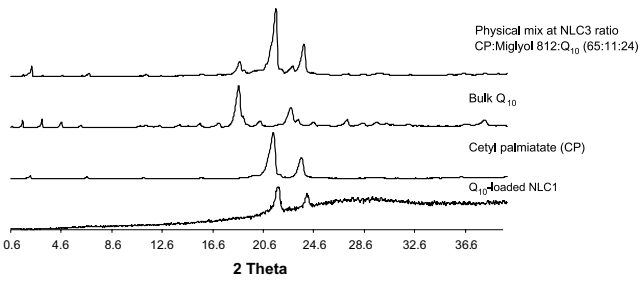

Fig. 3. X-ray diffraction patterns of Q_{10}-loaded NLC1, bulk cetyl palmitate, bulk Q_{10}, and the physical mixture based on NLC3 ratio.

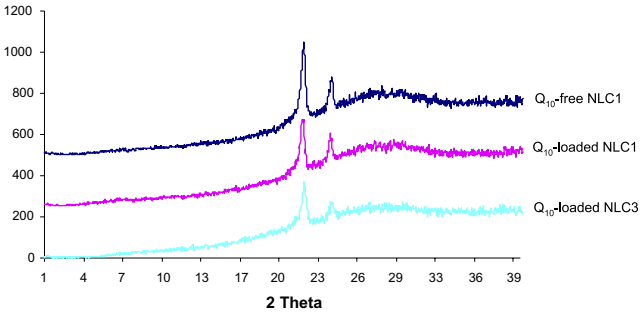

Fig. 4. X-ray diffraction patterns of Q_{10}-free NLC1, Q_{10}-loaded NLC1 and Q_{10}-loaded NLC3.

to the most stable polymorphic form (β) [18]. In general, the polymorphic forms of triacylglycerols (TAG) are in the α-, β′- and β-forms. An intermediate form (namely β_i) based on the subcell structures has been also reported [2,13]. However, in some mixed-acid TAG, which have saturated and unsaturated fatty acid moieties and/or containing fatty acids of different chain lengths, the main polymorphic form is the metastable form (β′) [29,30]. Concerning the physical mixture of cetyl palmitate and Q_{10} at the ratio of 76:24, the melting event of both cetyl palmitate and Q_{10} has been separately recorded (Fig. 2). Regarding the physical mixtures of three components based on NLC1 composition, it was found that it showed a melting peak of Q_{10}. The three component mixture based on NLC3 did not clearly show the melting event of Q_{10} because of the occurrence of a broadened peak (data not shown). These results support that Q_{10} is dissolved in the lipid matrix. During the production procedure, Q_{10} has been dissolved in the melted lipid phase. After cooling the dispersion to room temperature, the melting event of Q_{10} was not detected anymore. The absence of this melting event can be due to a super-cooled melted state, amorphous or molecular dispersed state of Q_{10} in the mixture (the latter confirmed by WAXS).

The melting point of NLC dispersions decreased with increasing the oil loading (Table 4). The crystallinity index (CI) of NLC dispersions was calculated using the Eq. (3) [31]. The CI decreased with the entrapment of Q_{10} and with the increase of the amount of oil, because of the enhancement of crystal disturbance within the lipid matrix of NLC. In case of NE, the melting event was obviously absent. Q_{10} was completely dissolved and no recrystallization of oil and/or active has been detected.

3.5. X-ray diffraction analysis

From the X-ray diffraction patterns shown in Fig. 3, it is confirmed that Q_{10} is molecularly dispersed (dissolved) in the blend of cetyl palmitate and Miglyol® 812, i.e. no peak of this active occurred in the NLC dispersion. Moreover, Q_{10}-loaded NLC revealed the typical reflections at 0.38 and 0.42 nm, which are characteristic of an orthorhombic subcell [25]. Thus, the active ingredient was maintained in between these layers [32].

Fig. 4 shows the diffractogram of Q_{10}-free NLC, Q_{10}-loaded NLC1 and Q_{10}-loaded NLC3. Comparing the active-free and active-loaded formulations a lower peak intensity was observed when Q_{10} was present and when increasing the oil loading. Therefore, the lower degree of crystallinity and the slight decrease of melting enthalpy recorded by DSC analysis of NLC dispersions are in agreement with the decrease of peak intensity observed by WAXS indicating a less ordered structure and pronounced crystal defects.

3.6. In vitro release studies

To elucidate the mechanism of active release from NLC for topical administration, *in vitro* release studies using vertical Franz diffusion cells have been performed. The temperature was controlled at 32 °C and the pH of the acceptor medium was approximately 5 corresponding to the skin surface condition. Because of the low solubility of Q_{10} in water and in buffer solution, in this study an aqueous solution of 5% Labrasol® (w/v) was selected as acceptor medium. Analysis of Q_{10} was performed over 24 h by HPLC at 280 nm, where the peak of Labrasol® does not interfere with the peak of Q_{10}. In this study, sink conditions were maintained over the experiments. The release profiles obtained from NLC were compared to those of NE (Fig. 5). The influence of particle size on the release profile of Q_{10} from NLC could be excluded because no major differences among the three NLC formulations (NLC1, NLC2 and NLC3) were observed ($p > 0.05$). Furthermore, the E.E. of all formulations was approximately 100%, and thus the occurrence of a fast release due to free

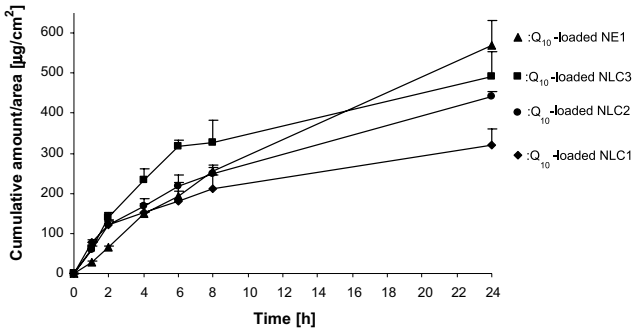

Fig. 5. Cumulative amount per unit area (μg/cm^2) of Q_{10} released from NLC and NE over a period of 24 h by Franz diffusion cells.

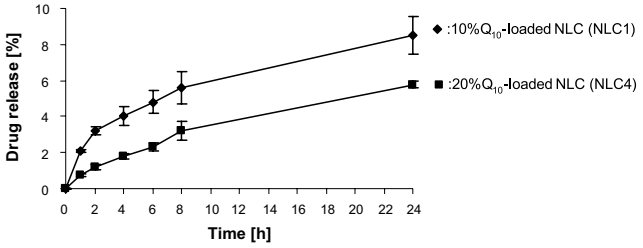

Fig. 6. Q_{10} release profiles from NLC formulations composed of 10% and 20% of lipid phase.

active in the dispersion could also be excluded. However, using one-way ANOVA comparing the difference in the mean particle size by PCS of Q_{10}-loaded NE and NLC, it was found that the particle size of Q_{10}-loaded NE was different from that of Q_{10}-loaded NLC formulations ($p < 0.05$).

Ten percentage of Q_{10}-loaded NLC1 dispersion revealed a faster release than NE at the initial stage, which was more pronounced with increasing amount of oil (NLC2 and NLC3), followed by a prolonged release. After 24 h, the cumulative amount released from NE was higher than those from all NLC dispersions. The release of Q_{10} from NE was almost constant, which could be explained by the Fick's law of diffusion. This principle cannot be, however, applied to explain the release mechanism of drug from NLC. The total content of lipid phase (cetyl palmitate, oil and Q_{10}) was identical for the Q_{10}-loaded NLC1, 2 and 3. The Q_{10} content was 2.4% for all three formulations, but the oil content increased from 0.38% to 0.76% and 1.14%.

The initial release within the first 2 h was higher for the NLC formulations than for the NE ($p < 0.05$) which can be explained by enrichment of Q_{10} in the outer shell of the particles. Enrichment in the outer shell was shown by AFM for Q_{10}-loaded SLN [3,33]. From our experiments, the release rate of Q_{10} from NLC containing 5%, 10% and 15% (w/w) of oils in the particle matrix (corresponding to 0.38%, 0.76% and 1.14% in total suspension) was dramatically reduced by approximately 40% after 4 (61.0 to 38.3 μg/cm^2/h), 6 (59.9 to 36.3 μg/cm^2/h), and 8 h (69.3 to 40.7 μg/cm^2/h), respectively. The prolonged release in the second phase and the lower total release after 24 h can be explained by slower diffusion of Q_{10} from the solid matrix of NLC. The solid lipid matrix has a higher viscosity, thus slowing down the release according to the law by Stokes–Einstein. The total amount release after 24 h increased from NLC1 to NLC3, which means with increasing oil content. By admixing oil the viscosity of the lipid particle matrix is reduced leading consequently to faster diffusion. Another explanation might be the inhomogeneity of the oil distributed within the inner structure of lipid matrices. The different melting behaviour of solid and liquid lipids can lead to accumulation of the liquid oil in the outer the shell of lipid nanoparticles after lipid crystallization. This oily layer contains also Q_{10}. As a result, a fast release at the initial stage of the assay has been observed [15]. Concerning the release model of NLC, it was found that the model to describe the release profile of Q_{10} from NLC is the Higuchi model.

Fig. 6 compares the drug release profiles between 10% and 20% of Q_{10}-loaded NLC (NLC1 and NLC4) to study the effect of the amount of lipid phase. The percentage of Q_{10} released from 20% dispersion was lower than that from 10% dispersion ($p < 0.05$) possibly because of the lower particle surface area of the 20% dispersion than the 10% dispersion owing to the bigger particle size of the 20% dispersion as mentioned earlier. Moreover, the effect of lipid concentration in SLN was also reported by Souto et al. [11] and it was explained based on the different morphological structures. A higher lipid concentration created the drug enriched core model which showed a prolonged release. From this study, it can be stated that it is possible to achieve the desired release profile by varying the solid lipid/oil ratio. The fast release at the initial stage of Q_{10}-loaded NLC appears to be suitable to promote Q_{10} penetration due to the higher concentration of free-Q_{10} at the skin surface after applying the formulation, and followed by the prolonged release to supply a certain level of Q_{10} in the skin. Moreover, film formation of NLC could lead to an increase in the occlusive effect enhancing the skin penetration.

4. Conclusions

NLC have proven to be suitable carriers for active pharmaceuticals especially for the topical route. These carriers demonstrated a good physical stability indicated by zeta potential value and a high entrapment efficiency value (almost 100%). The mean particle size of less than 250 nm assessed by PCS with a narrow size distribution (PI < 0.2) was found in all formulations. Zeta potential values higher than −40 mV were obtained indicating a good physical stability of colloidal dispersions. Concerning the effect of varying lipid and oil ratio on the mean particle size of NLC, no major difference was observed. However, increasing the amounts of oil loading led to a less ordered structure within the particles confirmed by DSC and X-ray diffractometry. It was found that NLC showed a biphasic release pattern, i.e. in comparison to NE, NLC provided

a fast release initially for skin saturation followed by a slow and prolonged release profile to maintain the skin concentration of Q_{10}. The most suitable model to describe the release profile of Q_{10} from NLC has been found to be the Higuchi model.

Acknowledgements

Financial support from the Thailand Research Fund (TRF) through the Royal Golden Jubilee Ph.D. Program (Grant No. PHD/0160/2546) and from the German Academic Exchange Service (DAAD) is gratefully acknowledged.

References

[1] W. Mehnert, K. Mäder, Solid lipid nanoparticles: production, characterization and applications, Adv. Drug Deliv. Rev. 47 (2001) 165–196.
[2] R.H. Müller, M. Radtke, S.A. Wissing, Nanostructured lipid matrices for improved microencapsulation of drugs, Int. J. Pharm. 242 (2002) 121–128.
[3] R.H. Müller, M. Radtke, S.A. Wissing, Solid lipid nanoparticles (SLN) and nanostructured lipid carriers (NLC) in cosmetic and dermatological preparations, Adv. Drug Deliv. Rev. 54 (2002) S131–S155.
[4] R. Alvarez-Román, A. Naik, Y.N. Kalia, R.H. Guy, H. Fessi, Skin penetration and distribution of polymeric nanoparticles, J. Control. Release 99 (2004) 53–62.
[5] R.H. Müller, C.M. Keck, Challenges and solutions for the delivery of biotech drugs-a review of drug nanocrystal technology and lipid nanoparticles, J. Biotechnol. 113 (2004) 151–170.
[6] S.H. Klang, M. Parnas, S. Benita, Emulsion as drug carriers-possibility, limitations and future perspectives, in: R.H. Müller, S. Benita, B. Böhm (Eds.), Emulsions and Nanosuspensions for the Formulation of Poorly Soluble Drugs, Wiley, London, 1998.
[7] R.N. Gursoy, S. Benita, Self-emulsifying drug delivery systems (SEDDS) for improved oral delivery of lipophilic drugs, Biomed. Pharmacother. 58 (2004) 173–182.
[8] V. Jenning, M. Schäfer-Korting, S. Gohla, Vitamin A-loaded solid lipid nanoparticles for topical use: drug release properties, J. Control. Release 66 (2000) 115–126.
[9] E.B. Souto, R.H. Müller, SLN and NLC for topical delivery of ketoconazole, J. Microencapsul. 22 (2005) 501–510.
[10] S.A. Wissing, R.H. Müller, Solid lipid nanoparticles as carrier for sunscreens: in vitro release and in vivo skin penetration, J. Control. Release 81 (2002) 225–233.
[11] E.B. Souto, S.A. Wissing, C.M. Barbosa, R.H. Müller, Development of a controlled release formulation based on SLN and NLC for topical clotrimazole delivery, Int. J. Pharm. 278 (2004) 71–77.
[12] E.B. Souto, R.H. Müller, Lipid nanoparticles in cosmetic and transdermal applications, in: D. Thassu, M. Deleers, Y. Pathak (Eds.), Nanoparticulate Drug Delivery Systems: Recent Trends and Emerging Technologies, CRC Press, Boca Raton, FL, 2006.
[13] R.H. Müller, K. Mäder, S. Gohla, Solid lipid nanoparticles (SLN) for controlled drug delivery – a review of the state of the art, Eur. J. Pharm. Biopharm. 50 (2000) 161–177.
[14] U. Hoppe, J. Bergemann, W. Diembeck, J. Ennen, S. Gohla, I. Harris, et al., Coenzyme Q10, a cutaneous antioxidant and energizer, Biofactors 9 (1999) 371–378.
[15] F.-Q. Hu, S.-P. Jiang, Y.-Z. Du, H. Yuan, Y.-Q. Ye, S. Zeng, Preparation and characterization of stearic acid nanostructured lipid carriers by solvent diffusion method in an aqueous system, Colloids Surf. B Biointerfaces 45 (2005) 167–173.
[16] V. Jenning, A.F. Thünemann, S.H. Gohla, Characterisation of a novel solid lipid nanoparticle carrier system based on binary mixtures of liquid and solid lipids, Int. J. Pharm. 199 (2000) 167–177.
[17] K. Jores, W. Mehnert, M. Drechsler, H. Bunjes, C. Johann, K. Mäder, Investigations on the structure of solid lipid nanoparticles (SLN) and oil-loaded solid lipid nanoparticles by photon correlation spectroscopy, field-flow fractionation and transmission electron microscopy, J. Control. Release 95 (2004) 217–227.
[18] A. Saupe, S. Wissing, A. Lenk, C. Schmidt, R.H. Müller, Solid lipid nanoparticles (SLN) and nanostructured lipid carriers (NLC) – structural investigations on two different carrier systems, Biomed. Mater. Eng. 15 (2005) 393–402.
[19] A. Saupe, K.C. Gordon, T. Rades, Structural investigations on nanoemulsions, solid lipid nanoparticles and nanostructured lipid carriers by cryo-field emission scanning electron microscopy and Raman spectroscopy, Int. J. Pharm. 314 (2006) 56–62.
[20] K. Westesen, B. Siekmann, M.H.J. Koch, Investigations on the physical state of lipid nanoparticles by synchrotron radiation X-ray diffraction, Int. J. Pharm. 93 (1993) 189–199.
[21] A. Dingler, R.P. Blum, H. Niehus, R.H. Müller, S. Gohla, Solid lipid nanoparticles (SLN™/Lipopearls™) – a pharmaceutical and cosmetic carrier for the application of vitamin E in dermal products, J. Microencapsul. 16 (1999) 751–767.
[22] D. Hou, C. Xie, K. Huang, C. Zhu, The production and characteristics of solid lipid nanoparticles (SLNs), Biomaterials 24 (2003) 1781–1785.
[23] M. Üner, S.A. Wissing, G. Yener, R.H. Müller, Solid lipid nanoparticles (SLN) and nanostrutured lipid carriers (NLC) for application of ascorbyl palmitate, Pharmazie 60 (2005) 577–582.
[24] A. zur Mühlen, C. Schwarz, W. Mehnert, Solid lipid nanoparticles (SLN) for controlled drug delivery – drug release and release mechanism, Eur. J. Pharm. Biopharm. 45 (1998) 149–155.
[25] V. Jenning, S.H. Gohla, Encapsulation of retinoids in solid lipid nanoparticles (SLN), J. Microencapsul. 18 (2001) 149–158.
[26] V. Jenning, S. Gohla, Comparison of wax and glyceride solid lipid nanoparticles (SLN®), Int. J. Pharm. 196 (2000) 219–222.
[27] K. Westesen, Novel lipid-based colloidal dispersions as potential drug administration systems-expectations and reality, Colloid Polym. Sci. 278 (2000) 608–618.
[28] C.H. Hsu, Z. Cui, R.J. Mumper, M. Jay, Preparation and characterization of novel coenzyme Q10 nanoparticles engineered from microemulsion precursors, AAPS Pharm. Sci. Technol. 4 (2003) E32.
[29] K. Sato, Crystallization behaviour of fats and lipids – a review, Chem. Eng. Sci. 56 (2001) 2255–2265.
[30] H. Bunjes, K. Westesen, H.J.K. Michel, Crystallization tendency and polymorphic transitions in triglyceride nanoparticles, Int. J. Pharm. 129 (1996) 159–173.
[31] C. Freitas, R.H. Müller, Correlation between long-term stability of solid lipid nanoparticles (SLN™) and crystallinity of the lipid phase, Eur. J. Pharm. Biopharm. 47 (1999) 125–132.
[32] G. Lukowski, J. Kasbohm, P. Pflegel, A. Illing, H. Wulff, Crystallographic investigation of cetylpalmitate solid lipid nanoparticles, Int. J. Pharm. 196 (2000) 201–205.
[33] A. Dingler, Feste Lipid-Nanopartikel als kolloidale Wirkstoffträgersysteme zur dermalen Applikation, PhD. Thesis, Freie Universität Berlin: Berlin, 1998.